Acoustic radiation by charged atomic particles in liquids: An analysis

John G. Learned*
University of California, Irvine, Irvine, California 92717
(Received 14 July 1978)

A new analysis of the propagation of acoustic pulses produced by local heating of liquids due to ionization by charged particles is presented. It is shown that the wave equations with loss dominate the pulse shape after small distances and that, due to the bipolar δ-function behavior of the individual pulses, a net observed pulse is just the time derivative of the received density of pulses from individual heating centers. Angular distributions, signal-to-noise ratios, detectable volume, and numerical examples are discussed. One important observation is that the effect of attenuation upon this type of radiation is to produce power-law rather than exponential cutoff with distance. For example, in the thermal-noise-limited case the signal-to-noise ratio defined herein only steepens by one-half power in falloff with distance due to attenuation.

INTRODUCTION

Substantial effort has been expended upon the problem of acoustic radiation from the local heating caused by the traversal of a charged particle or group of particles.[1-6] The heating takes place essentially instantaneously on both an acoustic and a thermal diffusion time scale. Herein the approach is taken that the bipolar nature of the pressure pulse emanating from a tiny heated region is known, but that detailed knowledge of its shape is not necessary beyond a normalization constant. It will be shown that the measurement of a macroscopic pulse arising from the sum of a large number of tiny pulses distributed in time permits calculation of this normalization constant for these individual microscopic source pulses. Once having measured the constant in question, one may proceed to calculate the pressure pulse from *any* given distribution of ionizing particles (assuming that they have the same mixture of δ rays that our first measurement has). One is able to calculate the magnitudes and angular distributions of pulses from showers of charged particles, and detectable volumes for them, for example.

An essential viewpoint of this paper, then, is that one need not be concerned with complex details on the atomic scale of the acoustic-pulse production, but that observation at finite distances yields signals whose character is controlled by the propagation constants of the medium. Considerable effort is required to solve the thermoacoustic equations on the microscopic scale, yet the details are unobservable except in special situations.

Another critical difference in approach taken herein, as compared with other published techniques for calculating particle-induced acoustic radiation, is the recognition of the importance of working in the time domain. Because of the impulsive nature of the source, the mathematics is simpler in the time domain and calculations using numerical techniques are not subject to the difficulties that appear when carrying out Fourier transforms for transient sources.

Since this work spans several areas of specialization in physics, some details, unnecessary to the expert, have been included and thus some readers may wish to skip sections. For example, Sec. I should not be necessary for those familiar with underwater acoustics. Section II presents some of the important characteristics of point-source radiation, many of which apply equally to distributed sources as shown in Sec. III. A specific geometry, that of line radiation including the effects of a finite distribution of ionization around tracks (such as those of relativistic heavy ions), is treated in Sec. IV. A short diversion in Sec. V demonstrates that the total acoustic noise resulting from cosmic-ray muons in the ocean is negligible compared to the thermal noise spectrum. Finally, in Sec. VI the problem of acoustic radiation from cascades of atomic particles is discussed and the results of an initial calculation presented.

It should be emphasized that throughout this paper I assume only the thermoacoustic production mechanism to be significant.

I. RADIATION FROM POINT SOURCES WITH ATTENUATION

The equations that govern the propagation of an acoustic pulse are three: equation of motion ($f=Ma$):

$$\rho_0 \dot{u}_x = -\frac{\partial p_e}{\partial x}, \tag{1}$$

equation of continuity (conservation of particles):

$$\rho_0 \frac{\partial u_x}{\partial x} = -\dot{\rho}_e, \tag{2}$$

equation of state (Stokes):

$$p_e = \rho_e \frac{K_s}{\rho_0} + \frac{\zeta}{\rho_0}\dot{\rho}_e, \tag{3}$$

where

ρ_0 = equilibrium density of the medium,

u_x = particle velocity in the x direction and the dot stands for time derivation (partial and total the same here),

p_e = the pressure, subscript e standing for excess over the equilibrium value,

K_s = the bulk compressibility of the medium,

ζ = a constant relating to the viscosity of the medium.

The equation of state is debatable. (A mechanical analog for this equation is a spring with parallel dashpot whose force is proportional to the velocity of the system. An electrical analog is a series LR circuit). One can choose other models (as for example Maxwell's equation),[7] but the simplest description of the observed loss in water and most liquids having a frequency-squared dependence is given by this model. An accurate predictive description does not exist on account of complex molecular relaxation phenomena in many liquids (particularly sea water) and because of small, but difficult to handle, thermal effects, shear effects, etc. The Stokes form will suffice for most situations, though, for example, the observed absorption is about $3\frac{1}{2}$ times the classic prediction above 1 MHz in water. We need only increase the absorption to match the observed value. The variation from frequency-squared dependence of the attenuation actually observed in the ocean provides the limitation for this model. It is not a serious limitation, however.

We may worry as to whether infinitesimal-amplitude acoustical theory applies here. Near the particle tracks it may not, where some shock-wave phenomena might need to be considered. The effect of a piling up of initial amplitude would be to introduce higher-harmonic content which would be severely attenuated by the medium, and hence unobservable.

The wave equation in terms of the pressure can be written

$$\nabla^2\left(p - \frac{1}{\omega_0}\dot{p}\right) - \frac{1}{c_0^2}\ddot{p} = 0\,, \tag{4}$$

where $\omega_0 = K_s/\zeta$ and $c_0 = (K_s/\rho_0)^{1/2}$. (In water $\omega_0 \approx 10^{12}$ Hz and $c_0 \approx 1.5\times10^5$ cm/sec.) This simple form will be adequate for our present requirements. (To appreciate the complex theoretical situation read Hunt's article on the propagation of sound in fluids[8] or Morse and Ingard's classic text,[9] Chap. 6.)

A useful approach to the solution of the wave equation is to take its Fourier transform

$$\nabla^2\left[\tilde{P}(x,\omega) + i\,\frac{\omega}{\omega_0}\,\tilde{P}(x,\omega)\right] + \left(\frac{\omega}{c_0}\right)^2 \tilde{P}(x,\omega) = 0\,, \tag{5}$$

where

$$\tilde{P}(x,\omega) = \int_{-\infty}^{\infty} p(x,t)e^{-i\omega t}dt\,. \tag{6}$$

Thus we can write

$$\nabla^2\tilde{P}(x,\omega) + k^2\tilde{P}(x,\omega) = 0\,, \tag{7}$$

where

$$k \equiv \pm\,\frac{\omega}{c}\,\frac{1}{(1+i\omega/\omega_0)^{1/2}}\,. \tag{8}$$

Then we immediately have solved the x dependence by

$$\tilde{P}(x,\omega) = \tilde{P}_0(\omega)e^{-ikx}\,. \tag{9}$$

Moreover, let us settle the question of radial dependence. In the case of a spherically symmetric source

$$\nabla^2 P = \frac{1}{r^2}\,\frac{\partial}{\partial r}\left(r^2\,\frac{\partial P}{\partial r}\right) = \frac{1}{r}\,\frac{\partial^2 P_r}{\partial r^2} \tag{10}$$

if we replace P by P_r/r.

We can also expand k since $\omega/\omega_0 \ll 1$:

$$k = \pm\frac{\omega}{c}\left[1 - \frac{3}{8}\left(\frac{\omega}{\omega_0}\right)^2 + \cdots\right] \mp i\,\frac{\omega^2}{2\omega_0 c}\left[1 - \frac{5}{8}\left(\frac{\omega}{\omega_0}\right)^2 + \cdots\right]\,.$$

We see that the dispersion will be slight for all the frequencies of interest to us (<100 MHz). So also will be the deviations from a frequency-squared dependence of the absorption term.

Keeping only the terms up to $O(\omega^2/\omega_0^2)$ we get

$$\tilde{P}(r,\omega) = \frac{1}{r}\,\tilde{P}_0(\omega)e^{-i(\omega/c)r - (\omega^2/2c\omega_0)r}\,. \tag{11}$$

So far we have only considered the source-free wave equation. Neglecting loss we can write the wave equation for a point source of heat[10] as

$$\nabla^2 p - \frac{1}{c_0^2}\,\ddot{p} = -\,\frac{\beta}{C_p}\,\frac{\partial E}{\partial t}\,, \tag{12}$$

where β is the bulk coefficient of thermal expansion, C_p is the specific heat at constant pressure, and E is the energy deposition in the form of heat. The solution to this is simply a pulse of the form of a time derivative of a δ function if we make the heat deposition a δ function in time and space:

$$E = E_0\delta(t)\delta(\vec{r})\,, \tag{13}$$

$$p(r,t) = \frac{E_0\beta}{4\pi C_p}\,\frac{\delta'(r/c - t)}{r}\,, \tag{14}$$

where r is a scalar quantity since this represents spherically symmetric monople radiation.

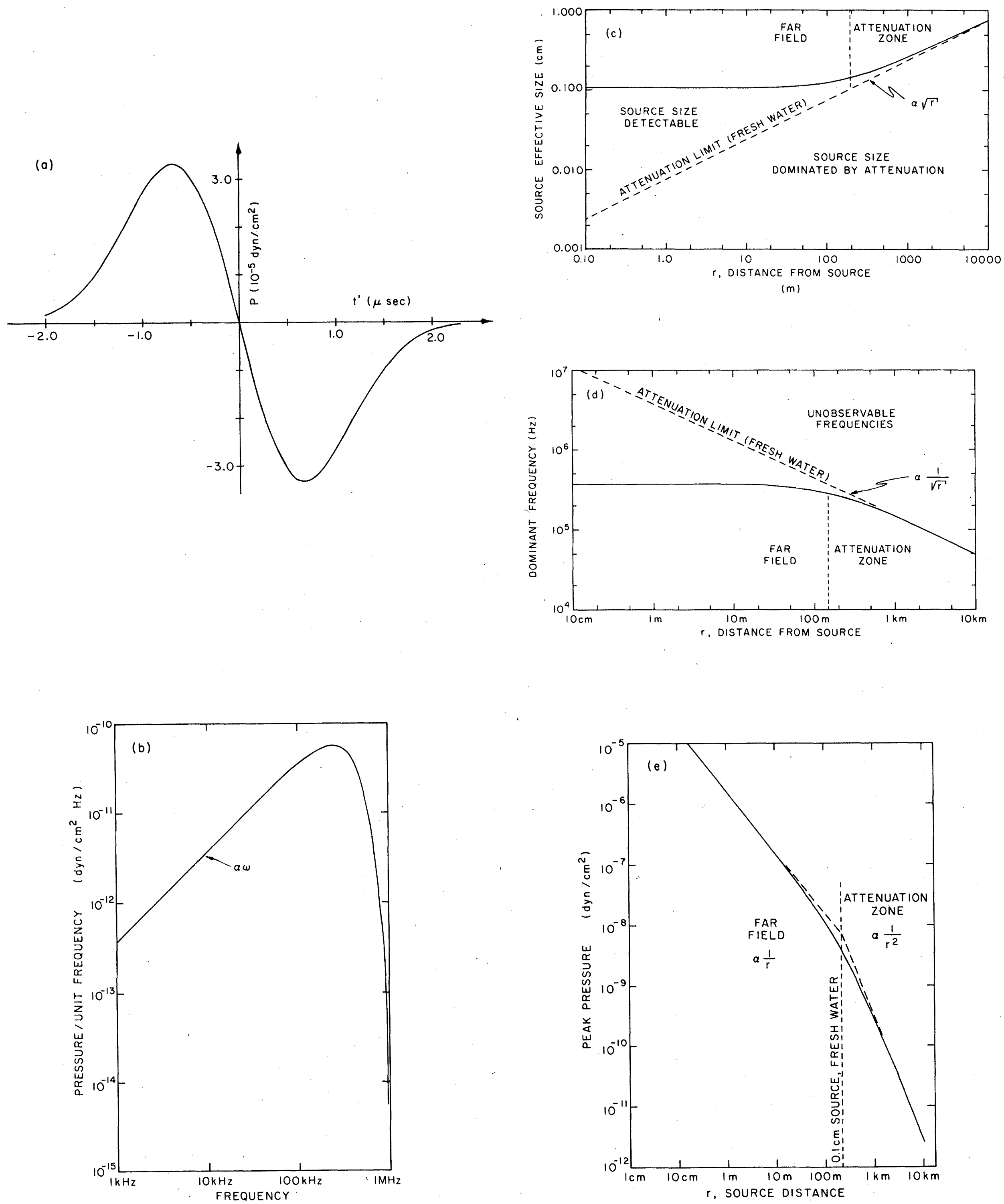

FIG. 1. Behavior of the radiation from a Gaussian deposition of heat. The magnitudes are given for fresh water at 20°C with a heat deposition of 2 GeV over a region with rms size of 1 mm. (a) The pressure pulse at 10-cm distance, (b) Fourier transform of pulse, and (c), (d), (e) variations of effective size, characteristic frequency, and maximum amplitude, respectively, with distance.

A more useful solution is for the case of a Gaussian distribution of heat

$$p(r\approx 0,t')=-\frac{AE_0}{r}\frac{t'}{\sqrt{2\pi}\,\sigma^3}\,e^{-(t'^2/\sigma^2)/2},\quad r>0,\quad (15)$$

where $A=\beta/4\pi C_p$, $t'=t-r/c$. This is a bipolar pulse, the time derivative of a Gaussian, which we will discuss further later on. It has Fourier transform (gotten by completing the square):

$$\tilde{p}_0=\tilde{p}(r\approx 0,\omega)=i\,\frac{AE_0}{r}\,\omega e^{-\sigma^2\omega^2/2}\,. \quad (16)$$

We now have the complete Fourier spectral function as a function of r, including attenuation [see Fig. 1(b)]:

$$\tilde{p}(r,\omega)=i\,\frac{AE_0}{r}\,\omega\exp-\left(i\frac{\omega r}{c}+\frac{\omega^2 r}{2\omega_0 c}+\frac{\sigma^2\omega^2}{2}\right). \quad (17)$$

To get the time dependence we retransform, arriving at

$$p(r,t')=-\frac{AE_0}{r}\frac{t'}{\sqrt{2\pi}\,\tau^3}\,e^{-t'^2/2\tau^2}\,, \quad (18)$$

where

$$t'=t-r/c\quad(t>0)$$

and

$$\tau=\left(\sigma^2+\frac{r}{\omega_0 c}\right)^{1/2}.$$

Notice that the function is the derivative of a Gaussian in time near the observation point (near zero in the retarded time) with a spread

$$\tau=\begin{cases}\sigma, & r\approx 0\\ \left(\dfrac{r}{c\omega_0}\right)^{1/2}, & r\text{ large }(\gg\omega_0 c\sigma^2)\end{cases}.$$

Explicitly writing the function in the limit of large r we have [see Fig. 1(a)]

$$p(r\text{ large},\ t')=-(\omega_0 c)^{3/2}\,\frac{AE_0}{\sqrt{2\pi}\,r^{5/2}}\,t'e^{-(\omega_0 c/2r)t'^2}\,. \quad (19)$$

This function has its extrema at

$$t_0'=\pm\left(\frac{r}{\omega_0 c}\right)^{1/2} \quad (20)$$

with value

$$|p_m(r\text{ large}|=\frac{\omega_0 c}{(2\pi e)^{1/2}}\,\frac{AE_0}{r^2}\,. \quad (21)$$

See the sketch in Fig. 1(e). This shows the effect of attenuation on an initially sharp pulse; the peak amplitude in the attenuation zone falls off as $1/r^2$ instead of $1/r$. This situation is vastly different from that encountered in the case of light, for example, where the attenuation of a source goes as the inverse square multiplied by an exponential. [The reason for comparison of field strength in the case of acoustics with intensity in the case of light is that real detectors (say hydrophones and phototubes) generally produce output amplitudes proportional to the field strength in the acoustics case (coherent pressure sensing) and light intensity (incoherent photon collection).] The cutoff in this acoustic case is far more gentle, being a power law. Notice also that the bandwidth will decrease slowly, as $1/\sqrt{r}$ [see Figs. 1(c) and 1(d)].

II. CHARACTERISTICS OF POINT-SOURCE RADIATION

Let us examine several integral quantities. The impulse may be defined as

$$2\int_0^\infty |p(r,t)|\,dt=\left(\frac{2}{\pi}\right)^{1/2}\frac{AE_0}{r}\,\frac{1}{\tau}\,. \quad (22)$$

Thus the impulse at first falls as $1/r$ and then faster as $1/r^{3/2}$. Another integral of interest is the total radiated energy flux

$$\begin{aligned}E_T(r)&=\frac{4\pi r^2}{\rho c}\int_{-\infty}^{\infty}p^2(r,t)\,dt\\&=\frac{\sqrt{\pi}A^2E_0^{\,2}}{\rho c}\,\frac{1}{\tau^3}\,.\end{aligned} \quad (23)$$

We see that the pulse energy falls off as $r^{-3/2}$, integrated over the sphere, which represents energy dissipated by the viscosity of the fluid (and other mechanisms).

Another quantity of interest is the first moment of the pulse

$$\int_{-\infty}^{\infty}tp(r,t)dt=-\frac{AE_0}{r} \quad (24)$$

at all distances. This integral does not suffer the attenuation effects. Bowen made the same observation,[4] but arrived at it in a rather different way. (We can identify this integral with his J_r and find the same value for A as deduced from the δ-function solution.)

It is worth noting that the efficiency for acoustic energy radiation using Eq. (23) is

$$\begin{aligned}\epsilon_0\equiv\frac{E_T(r\approx 0)}{E_0}&=\frac{c^2\beta^2}{16\pi^{3/2}\rho C_p^{\,2}}\,\frac{E_0}{(\sigma c)^3}\\&\approx 9\times 10^{-9}\,\frac{E_0\ (\text{MeV})}{[\sigma c\ (\mu\text{m})]^3}\,,\end{aligned} \quad (25)$$

where the numerical value (typical) is given for fresh water at 20℃ (see list of properties in Table I). Notice that the efficiency ϵ_0 depends upon the energy per unit volume where σc characterizes the

TABLE I. Various constants relating to acoustic signal production and propagation, as discussed in the text. The last column can be taken as a figure of merit for various production media in the case of acoustic radiation by a charged-particle beam of fixed dimensions. The constants come largely from Refs. 8 and 22, as well as several others (especially Ref. 23). Since some of the values have been estimated and/or extrapolated from other conditions, it is only safe to assume these numbers as representative (to about ±10%).

Class	Substance Name	Symbol	Temperature T (°C)	Density ρ (g/cm^3)	Velocity of sound c_s (10^5 cm/sec)	Coefficient of attenuation for sound $a=\alpha/f^2$ (10^{-15} sec^2/cm)	Molecular weight M (g/mol)	Volume expansivity β (10^{-3}/°C)	Specific heat at constant pressure C_p (10^{10} MeV/g °C)	Minimum energy loss rate dE/dk (MeV cm^2/g)	$\frac{c^2\beta\rho \frac{dE}{dx}}{C_p}$ (10^{-6} g/sec^2)
Organics											
Alcohols	Methanol	CH_4O	20	0.7914	1.121	0.302	32.04	1.170	1588.0	2.06	1.51
	Ethanol	C_2H_6O	20	0.7893	1.162	0.485	46.07	1.199	1530.0	2.12	1.77
	n-propyl	C_3H_8O	20	0.8035	1.223	0.645	60.11		1488.0	2.12	
	n-butyl	C_4H_9O	20	0.7887	1.258	0.743	74.12		1462.0	2.10	
Alkanes	n-penthane	$n-C_5H_{12}$	20	0.626	1.008	10	72.15	1.608	1423.0	2.21	1.59
	n-hexane	$n-C_6H_{14}$	20	0.660	1.083		86.18		1411.0	2.20	
	n-heptane	$n-C_7H_{16}$	20	0.684	1.162		100.20		1399.0	2.20	
	n-octane	$n-C_8H_{18}$	20	0.703	1.197		114.23		1387.0	2.19	
Benzenes	Benzene	C_6H_6	20	0.879	1.295	8.73	78.12	1.237	1082.0	1.72	2.90
	Fluoro-	C_6H_5F	20	1.023	1.183	3.17	96.11		953.0	1.93	
	Chloro-	C_6H_5Cl	20	1.106	1.311	1.67	112.56		809.0	1.85	
	Bromo-	C_6H_5Br	20	1.495	1.169	1.63	157.02		617.0	1.67	
	Iodo-	C_6H_5I	20	1.831	1.114	2.42	204.01			1/53	
Other	Carbon disulfide	CS_2	20	1.263	1.140	56.80	76.14	1.218	624.0	1.59	5.09
	Acetone	C_3H_6O	20	0.7899	1.203	12.03	58.08	1.487	1357.0	2.06	2.58
	Carbon tetrachloride	CCl_4	20	1.594	0.926	5.38	153.82	1.236	525.0	1.64	5.28
	Chloroform	$CHCl_3$	20	1.483	0.987		119.38	1.273	603.0	1.66	5.06
	Glycerol	$C_3H_3O_3$	20	1.261	1.904		92.10	0.505	1618.0	2.01	2.87
	Freon 13 $B1$	CF_3Br	28 (9 atm)	1.50			148.92		1054.0	1.52	
	Propane	C_3H_8	57 (9 atm)	0.41			44.11		1372.0	2.28	
	Ethylene glycol	$C_2H_6O_2$	20	1.117	1.669		62.07		1514.0	2.03	
Diatomic	Hydrogen	H_2	26 °K	0.0708	1.200	0.056	2.016	14.6	8053.0	4.12	0.76
	Nitrogen	N_2	77 °K	0.808	0.962	0.106	28.01	5.8	1273.0	1.82	6.18
	Oxygen	O_2	99 °K	1.144	0.913	0.086	32.00	4.2	1060.0	1.80	6.80
	Fluorine	F_2	85 °K	1.108			38.00		931.0	1.76	
	Chlorine	Cl_2	−33.7	1.568			70.91		587.0	1.60	
	Bromine	Br_2	20	3.12	0.716		159.8	1.132	294.0	1.40	8.62
Noble	Helium	He	4.2 °K	0.125	0.180	2.60	4.00	168.0	2688.0	1.94	0.49
	Neon	Ne	27 °K	1.204			20.18		1151.0	1.73	
	Argon	A	87 °K	1.394	0.853	0.101	39.95	4.65	687.0	1.51	10.37
	Krypton	Kr	120 °K	2.412			83.80		334.1	1.39	
	Xenon	Xe	166 °K	3.063			131.30		211.7	1.28	
Other	Mercury	Hg	20	13.546	1.451	0.064	200.6	0.18175	86.9	1.13	67.40
	Water, distilled	H_2O	20	0.998	1.483	0.253	18.02	0.207	2610.0	2.03	0.35
	Water [a], Sea (S=3.5%)	$H_2O+NaCl+$	1.5	1.051	1.52		18.02	0.117	2371.0	2.03	0.25
	Air (gas)	N_2+O_2+	20	0.001205	0.343		28.96		636.0	1.82	

[a] Depth of 5 km.

initial deposition region. It is also perhaps worth noting that if $\sigma c = 1$ Å and E_0 is in the range 100 eV the efficiency can be very high (though these equations are not sensible for that case). But at large distances the apparent efficiency will be

$$\epsilon_r \equiv \frac{E_T(r)}{E_0} = \frac{c^{1/2}\omega_0^{3/2}\beta^2}{16\pi^{3/2}\rho C_p^2}\,\frac{E_0}{r^{3/2}}$$

$$\approx 10^{-10}\,\frac{E_0\,(\mathrm{MeV})}{r^{3/2}\,(\mathrm{cm})}\,. \qquad (26)$$

As expected, the parameters of the deposition region no longer appear (so long as they are small). This efficiency roughly agrees with other estimates.[6] Causing the deposition to be highly localized makes the microscopic efficiency high, but at large distances it is only the total energy deposited that controls the radiation efficiency (as long as the deposition region size is large compared to the attenuation cutoff wavelength.)

Another set of integrals has to do with the signal to-noise ratios. Signal-to-noise ratios are defined and calculated in various ways.[11] Ultimately in our case one wants to calculate a quantity that represents the scale factor in a probability distribution for noise faking a signal. One measure of this that will suffice for preliminary estimates is the ratio of instantaneous signal voltage to rms noise voltage at the output of a hypothetical optimal filter attached to the output of an ideal transducer. An optimal filter is one which will maximize the "distance" between noise and signal in some space (the analogy can be made rigorously). The standard recipe in electrical engineering is to "prewhiten the noise" and then use a "matched filter." One can think of scaling arriving signals to the noise basis set and then measuring their projection along the vector pointing in the direction of the desired signal. The noise power in a three-dimensional medium has a frequency dependence proportional to the number of available states, which goes as the square of the frequency times the bandwidth.[12] The signal-to-noise ratio[13] can be written

$$S/N \equiv \int_{-\infty}^{\infty} dt\, I^2(r,t)/KT\rho/2\pi c$$

$$= \frac{\beta^2 c E_0^2}{8\pi C_p^2 \rho k T r^2}\int_{-\infty}^{\infty} S^2(t)\,dt$$

$$= \frac{\beta^2 c}{16\pi^{3/2} C_p^2 \rho k T}\,\frac{E_0^2}{r^2\tau}\,, \qquad (27)$$

$$I(r,t) \equiv \int_{-\infty}^{t} dt'\, p(r,t')\,, \qquad (28)$$

for a Gaussian source distribution [Eq. (18)]. Because τ becomes dominated by the attenuation factor at large distances, the distance dependence goes to

$$S/N \propto r^{-5/2}\,, \quad r \gg \sigma^2\omega_0 c\,.$$

The interesting result, which may have important implications for the DUMAND (Deep Underwater Muon and Neutrino Detector) project then is that *attenuation only adds one-half power falloff in distance* and, again, *not* an exponential cutoff (as long as the noise power has thermal, or frequency-squared, behavior).

Another observation that will prove useful later is that since the effect of attenuation in the frequency domain is to multiply by a Gaussian in frequency, we can equivalently account for the attenuation effects by convoluting any pressure pulse with the Fourier transform of the loss function. We shall call this a smearing function and it can be written as

$$Q(t) \equiv \left(\frac{\omega_0 c}{2\pi r}\right)^{1/2} e^{-\omega_0 c t^2/2r}\,. \qquad (29)$$

Summarizing results up to this point: We have formed a microscopic test pulse, a bipolar Gaussian derivative, propagated it in accordance with Stokes's equation and found that the time dependence was controlled by the medium after small distances. Moreover, we have identified several integrals and their radial dependences, and via the first moment of the pulse have established a connection with the detailed theory of Bowen, demonstrating the independence of the normalization constant from the details of the solution to the thermoacoustic equations. We have also observed the remarkably small effect of attenuation upon these kinds of pulses.

III. COMBINING POINT SOURCES IN THE TIME DOMAIN

It will prove useful to have the following identity for finding the pressure pulse $[P(r,t)]$ arising from the sum of many point sources:

$$P(r,t) = \text{constants} \times \frac{\partial}{\partial t}\, s(t)\,, \qquad (30)$$

where $S(t)$ is the density of sources as projected to the observation point r. Think of folding all the sources onto one line r and arrival times t,

$$S(t) = \int dV\, \rho(r,t)\,\delta(r-ct)\,, \qquad (31)$$

where the integral is over the whole energy deposition range and where r is measured from the observation point. Now the trick is simply that the very short individual pulses differentiate the distribution function $[S(t)]$. To prove this we first take the convolution of individual pulses and the density function

$$P(r,t) = \int_{-\infty}^{\infty} dt'\, S(t-t')\,p(r,t')\,. \qquad (32)$$

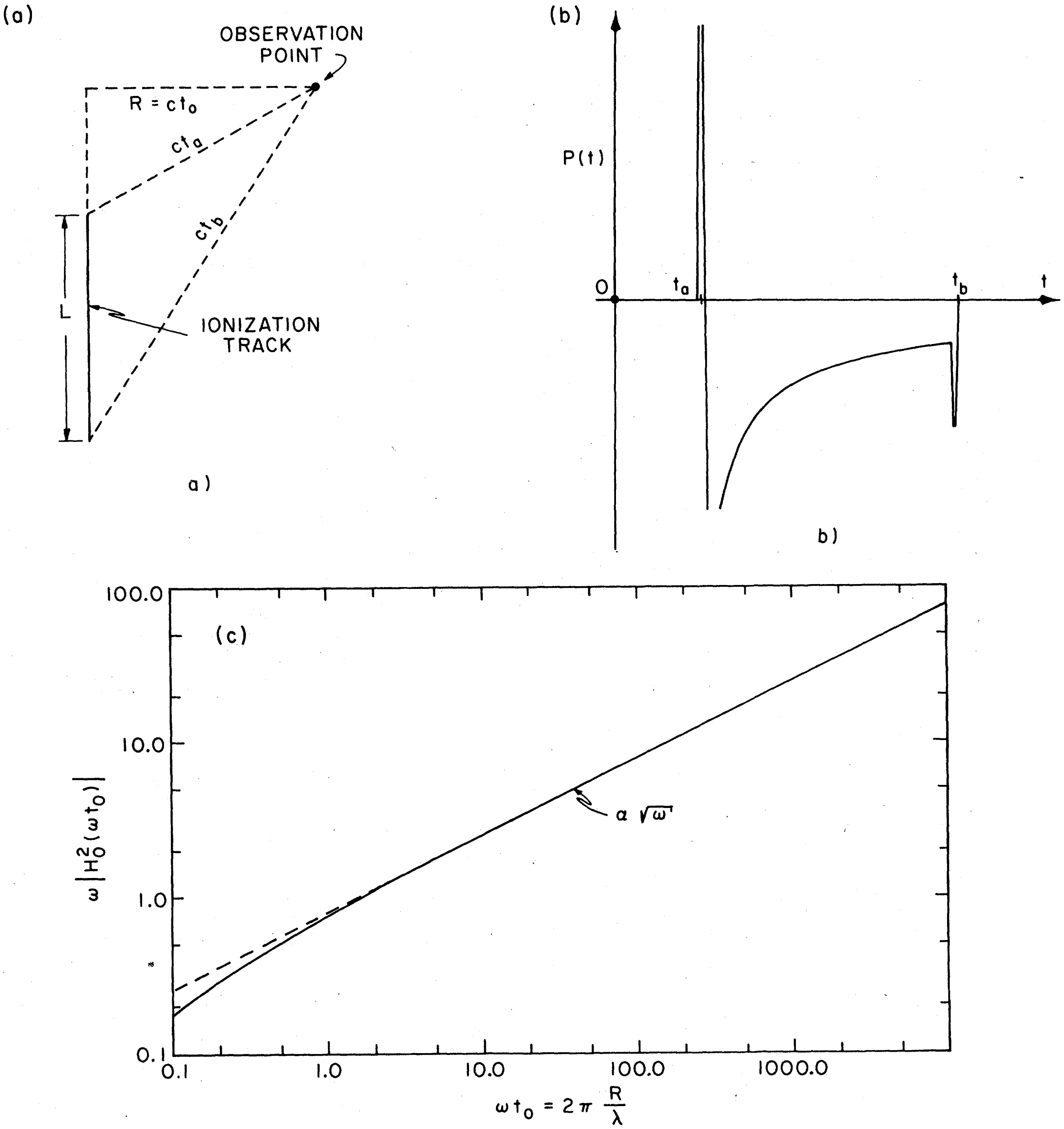

FIG. 2. Radiation from a line distribution. (a) Shows geometry for observer at perpendicular distance R from track of length L, beginning at time t_a and ending at time t_b as heard by the observer (deposition at $t=0$). (b) Contains a sketch of the time behavior of the pressure pulse from such a distribution. In (c) the Fourier transform exhibits greater than linear frequency dependence at very low frequencies ($\omega \ln \omega$) and a slow growth at typical high frequencies ($\sqrt{\omega}$).

This has Fourier transform

$$\tilde{p}(r,\omega)=\tilde{S}(\omega)\tilde{p}(r,\omega)\,. \tag{33}$$

If the pulse is sufficiently short, which is to say short compared to the granularity of the distribution function, we can replace $\tilde{P}(r,\omega)$ by the time derivative of a δ function:

$$\mathfrak{F}\left[\frac{\partial}{\partial t}\,\delta\left(t-\frac{r}{c}\right)\right]=i\omega e^{-i\omega r/c}\,. \tag{34}$$

Examining the spectrum of a given pulse [e.g., Eq. (17)] we see that this is quite justified in general, if

$$\omega<\left(\frac{2c\omega_0}{r}\right)^{1/2} \tag{35}$$

(i.e., <1 MHz even at an r of 1 km for water).

It is well known that multiplication of the Fourier transform of a function by $i\omega$ is equivalent to differentiation in the time domain. Thus, the result is

$$P(r,t)=AE\,\frac{\partial}{\partial t}\left[\frac{s(t)}{r}\right]. \tag{36}$$

Now we can see the importance of the parameter A. If we use this theorem to measure A, given that we know the dimensions of a burst of particles, then we both check the validity of the simple thermoacoustic theory, and we may calculate back to a single pulse and forward again to any distribution. One measurement should, in principle, specify all further results. Using the numbers given previously, Eq. (36) takes the value for fresh water at 20℃ of

$$P(r,t)=6\times10^{-25}E\,\frac{\partial}{\partial t}\left[\frac{s(t)}{r}\right], \tag{37}$$

where P is in dyn/cm², E is in eV, and r is in cm. The r has been left inside the time derivative to account for the special case of an extended distribution, wherein the amplitudes of the micropulses vary across the distribution of tracks (see Sec. IV). (With the integral of s normalized to unity we can set E equal to the total energy deposition.) Observe that the first moment of the micropulse is conserved in this case as well [Eq. (28)]:

$$\int_{-\infty}^{\infty} tP(r,t)dt=AE\int t\,\frac{\partial}{\partial t}\left(\frac{s}{r}\right)dt$$
$$=-\frac{AE}{r}, \tag{38}$$

but only if r does not vary significantly over the distribution arrival time (though even then it works if one chooses an appropriate r). We might observe that the total radiated energy [Eq. (23)] is not independent of $s(t)$, but is obviously maximized by a δ-function distribution.

A word of caution should be added about the use of Eqs. (36) and (37) in the cases where the source size is small. One will have to take account then of the stronger r dependence ($-\frac{5}{2}$ power) of short pulses, as given by Eq. (19). Mathematically, we would have to do the convolution using the smearing function [Eq. (29)]. Practically, it will be of consequence for sources of centimeter size observed from greater than kilometer distances in water.

One of the most important distributions we shall encounter is the Gaussian (either two or three dimensional which project as a one-dimensional Gaussian, or even four dimensional if there is a Gaussian particle pulse distribution in time, as at an accelerator. For the time distribution we simply convolute with the spatial distribution, the mean square deviations in time being added.) The Gaussian distribution as illustrated in Fig. 2(a) leads to a pressure pulse

$$P(r,t')=-\frac{AE}{r}\,\frac{t'}{\sqrt{2\pi}\,\tau^3}\,e^{-t'^2/2\tau^2}. \tag{39}$$

At maximum this pulse has a value of

$$|P_m|\approx 7.4\times10^{-26}\frac{E}{r\sigma^2}, \tag{40}$$

for P_m in dyn/cm², E in eV, r in cm, and σ in sec, where, again, the numerical example is for fresh water at 20℃ (see Table I). Note that we have come full circle. Equation (39) is identical with the micropulse expression in Eq. (18). Thus the equations for the "micropulse" apply for the "macropulse" as well, in particular, Eqs. (19)–(21) giving the effect of attenuation, and Eq. (28), expressing the effect of distance upon the signal-to-noise ratio.

IV. LINE DISTRIBUTION

We will now discuss the acoustic radiation from a line source of ionization such as that produced by a single charged particle moving in an essentially straight line. First let us consider the case of a δ function of ionization along the track. The pressure pulse for this case is gotten from

$$\frac{S(t)}{r}=\frac{1}{L(t^2-t_0^2)^{1/2}}\left[u(t-t_a)-u(t-t_b)\right], \tag{41}$$

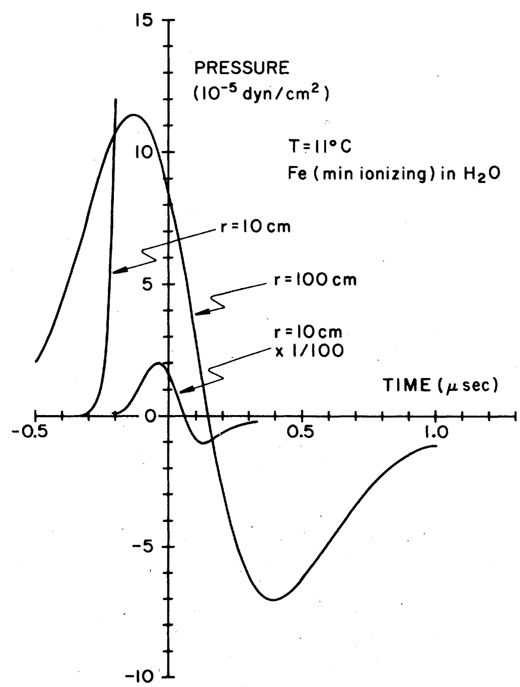

FIG. 3. Pressure pulse from a relativistic iron nucleus traversing water, as seen at several distances.

where

$t_0 = R/c$,

$u(x) = 0, \quad x < 0, 1, \quad x > 0$,

$E = L dE/dx$,

and the sketch [Fig. 2(a)] shows the other parameters. The pressure is then

$$P(t) = A \frac{dE}{dx} \left\{ 1/(t^2 - t_0^2)^{1/2} [\delta(t - t_a) - \delta(t - t_b)] - \frac{t}{(t^2 - t_0^2)^{3/2}} [u(t - t_a) - u(t - t_b)] \right\}. \quad (42)$$

This function, as illustrated in Fig. 2(b), consists of a large compression spike followed by a smaller rarefaction pulse with a long tail. This is typical of the solution to a two-dimensional wave equation: One finds functions that are asymmetric in space. The Fourier transform can be easily obtained by observing that

$$\tilde{P}(\omega) = AE \int_{-\infty}^{\infty} \frac{\partial}{\partial t}\left(\frac{S}{r}\right) e^{i\omega t}\, dt$$

$$= -i\omega AE \int_{-\infty}^{\infty} \frac{S(t)}{ct} e^{i\omega t}\, dt$$

$$= -i\omega A \frac{dE}{dx} \int_{-\infty}^{\infty} dt \frac{e^{i\omega t}}{(t^2 - t_0^2)^{1/2}} \times [u(t - t_a) - u(t - t_b)]$$

$$= -i\omega A \frac{dE}{dx} \int_{\cosh^{-1}(t_a/t_0)}^{\cosh^{-1}(t_b/t_0)} d\theta\, e^{i\omega t \cosh(\theta)}.$$

This integral has a simple form when $t_a = t_0$ and $t_b \to \infty$:

$$\tilde{P}(\omega) = \frac{\pi\omega A}{2} \frac{dE}{dx} H_0^2(\omega t_0), \quad (44)$$

where H_0^2 is the Hankel function of the second kind. In the case where observations are made at many wavelengths from the track the behavior is

$$\tilde{P}(\omega) \approx \left(\frac{\pi\omega}{2t_0}\right)^{1/2} A \frac{dE}{dx} e^{i(\omega t_0 - \pi/4)}, \quad \omega t_0 \gg 1 \quad (45)$$

while in the low-frequency region the behavior is stronger with frequency:

$$\tilde{P}(\omega) \approx -i\omega \ln(\omega t_0) A \frac{dE}{dx}, \quad \omega t_0 \ll 1. \quad (46)$$

This is illustrated in Fig. 2(c). It is interesting, but not surprising, to note that the same solution can be obtained by starting with the two-dimensional wave equation.

In order to account for the effects of attenuation of the medium we may convolute the pressure as a function of time [Eq. (42)] with the smearing function [Eq. (29)]. The smearing function, of course, transforms the compression peak to a Gaussian, but the rarefaction is more difficult. The pulse from a finite line source becomes more symmetrical with distance until it can be treated as a point (when its projected length becomes small compared to the minimum observation wavelength). A more realistic model of the distribution of ionization around a single track is given by[14]

$$\frac{dE}{dV} = \frac{dE}{dx}\left[0.5\delta(\rho) + 0.5 \frac{\rho_0^2}{(\rho + \rho_0)^2} e^{-\rho^2/2\rho_m^2}\right], \quad (47)$$

where

$\rho_0 \approx 1\ \mu\text{m}$,

$\rho_M \approx 0.6 R_e(T_m)$,

$\frac{dE}{dx} \approx -\rho Z_p^2 \frac{Z_m}{A_m} \frac{1}{\beta^2} \times$constants$\times$log terms

= energy loss per unit distance in the medium,

$R_e(T_m)$ = range of an electron with the maximum δ-ray energy $[T_m \approx 2m_e(P_p/m_p)^2]$,

Z_p = charge of the particle,

Z_m/A_m = average of charge-to-atomic-number ratio of elements of the medium (by fractional density),

ρ_m = density of the medium.

One sees that the resultant pressure pulse will be sensitive to the details of this distribution, particularly the parameter ρ_M which governs the low-frequency content. Explorations of the acoustic radiation at high frequencies could prove to be a useful tool for investigating the ionization distribution around heavy ions, a subject which has played an important role in the detection of ultraheavies and a claimed discovery of a magnetic monopole in cosmic rays (Ref. 14).

In order to examine the pressure pulse from more realistic circumstances, a program has been written which numerically intergrates the ionization from a given spatial distribution, generating the $s(t)$ function. It then calculates the pressure pulse and convolutes with the smearing function to account for attenuation. Values are calculated for various integrals, including the theoretical maximum signal-to-noise ratio, and the pulse is Fourier transformed. This program was used to calculate the pressure pulses illustrated in Fig. 3 for fresh water at 20℃ with a relativistic iron nucleus as the source, as observed at several distances from the track. The temporal nature of pulses appears similar for various media, results of which are summarized in Table II. We see that

TABLE II. Results of computer calculations for the pressure wave created by iron nuclei of 1.9 GeV/nucleon in the liquids indicated. The resulting signal-to-noise ratios assume an infinite medium and thermal noise limited detection system. The last three columns show the effect of localizing tracks to a 2-mm rms diameter region. Distance is 10 cm.

			Single track			2-mm beam diameter		
Material	T (°C)	dE/dx (MeV/cm)	f_p (kHz)	S/N (dB)	$\lvert P_m\rvert$ (10^{-3} dynes/cm^2)	f_p (kHz)	S/N (dB)	$\lvert P_m\rvert$ (10^{-3} dynes/cm^2)
CCl_4	25	2190	663	−27.4	9.94	193	−27.3	1.53
H_2O	11	1670	2929	−59.2	1.44	311	−58.8	0.053
Hg	25	13430	5823	−18.1	1751.00	302	−17.6	22.5
CS_2	25	967	204	−32.8	0.710	158	−32.4	0.497
Acetone	25	1318	443	−33.0	1.71	212	−32.9	0.613
Benzene	25	1420	520	−31.5	2.57	237	−31.4	0.861
Liquid argon	−186	686	4635	−15.3	391.00	178	−14.7	3.22

substantial gains over water can be appreciated in terms of pressure very near the source, but that attenuation takes most of this back for reasonable distances (e.g., centimeter distances for track detectors). Further work is required for solid materials and gases.

V. TOTAL NOISE IN THE OCEAN

It is amusing to calculate the total amount of noise produced by cosmic rays[18] in the ocean. A short calculation follows, yielding an upper limit. Let us assume that all the energy of cosmic rays arrives randomly at the ocean surface and is deposited in packets, whose dimensions we need not be concerned with so long as the dimensions of the distribution are small compared to the wavelengths at which we make observations. This produces an upper limit because (for an average muon track with energy 2×10^9 eV and actual range of 10 m) we are assuming that the energy is deposited in a small region, say 1 cm, and therefore has much greater (10^3) acoustic radiation efficiency. If the observation is made at a depth h the total noise received from cosmic rays can be gotten by integrating the received energy from each event (incoherent addition):

$$\begin{aligned} I(\omega) &= \int_{-\infty}^{\infty} 2\pi\rho d\rho I(r,\omega) = \frac{2\pi}{\rho c}\int \tilde{P}^2(r,\omega)\rho d\rho \\ &= \frac{2\pi A^2 E_0{}^2\omega^2}{\rho c} I_0 e^{-\sigma^2\omega^2} \\ &\quad\times \int_0^{\infty} \frac{\rho d\rho \exp[-(\omega^2/\omega_0 c)(\rho^2+h^2)^{1/2}]}{\rho^2+h^2} \\ &= \frac{2\pi A^2 E_0{}^2\omega^2 I_0}{\rho c}\,\frac{e^{-\omega^2(\sigma^2+h/\omega_0 c)}}{(1+\omega^2 h/\omega_0 c)^2}, \end{aligned} \tag{48}$$

where I have used Eq. (17) for the spectral density, where $\rho=(r^2+h^2)^{1/2}$, where I_0 is the cosmic-ray flux per unit area, and where E_0 is the average cosmic-ray energy at sea level. In the low-frequency limit (which again overestimates the noise) we then have

$$I(\omega) \approx \frac{2\pi A^2 E_0{}^2\omega^2 I_0}{\rho c}. \tag{49}$$

Now the minimum noise in the ocean,[12] arising from the random thermal motions of the medium is given by

$$N(\omega) = kT\,\frac{4\pi f^2}{c^2}\,df. \tag{50}$$

The ratio of cosmic-ray-produced noise to thermal noise power is then

$$\frac{I}{N} \ll \frac{c\beta^3 E_0{}^2 I_0}{8C_p{}^2\rho kT} \approx 7\times10^{-13}, \tag{51}$$

and thus negligible. This may, however, be misleading because though the average noise is small, some phase information has been neglected. A more sophisticated calculation is required to examine the possibility of significant rate (above random fluctuations) of pulses arriving from distant muons of great energy that penetrate to the ocean bottom, radiating relatively large amounts of acoustic energy. To estimate this rate let us assume that all muons arrive vertically and that the ocean is a homogeneous medium of constant depth and infinite extent. The average ocean depth is about 4 km (Ref. 15) and the rate of cosmic-ray muons reaching this depth is approximately $I_0=70/$km^2 sec.[16] The energy lost in reaching this depth is about $E_{min}=3$ TeV. The average energy loss rate is rising linearly in this region and is at a rate of about 4 TeV/km at 10-TeV energy.[17] We can thus assume an energy-loss spectrum that goes as

$$\begin{aligned} \frac{d^3I}{dE\,dA} &= \frac{I_0}{(\gamma-1)E_{min}}\left(\frac{E}{E_{min}}\right)^{-\gamma}, \\ \frac{d^2I}{dA} &= I_0\left(\frac{E}{E_{min}}\right)^{-\gamma+1}, \end{aligned} \tag{52}$$

where γ is the differential muon surface spectrum (~3.7).[18]

The maximum signal-to-noise ratio for distant pulses is given by Eq. (28):

$$S/N = \frac{\sqrt{\omega_0}\, d^{3/2}\beta^2 E^2}{16\pi^{3/2} C_p{}^2 \rho k T r^{3/2}} \equiv \alpha \frac{E^2}{r^{5/2}} ,\quad \alpha \approx 8.5\times 10^{-29}\ \mathrm{cm}^{5/2}/\mathrm{eV}^2 . \tag{53}$$

If we fix a minimum signal-to-noise ratio then we can solve for the energy required to produce a signal of that level at that distance:

$$E_{\mathrm{TH}} = \left(\frac{S/N}{\alpha}\right)^{1/2} r^{5/4} . \tag{54}$$

The rate of events producing pulses above the threshold S/N ratio will then be

$$R = \int_{r_{\min}}^{\infty} 2\pi r\, dr\, r^{-5/4(\gamma-1)} I_0 \left(\frac{S/N}{\alpha E_{\min}}\right)^{-\gamma+1} , \tag{55}$$

where $r_{\min} = (\alpha/S/N)^{2/5} E_{\min}{}^{4/5}$. We see that the integral does not diverge with distance; the gain in rate due to increasing area is overwhelmed by the steep spectrum. This conclusion can change if (due to direct muon production at the primary cosmic-ray interaction and other possibilities) the spectrum should become flatter at very high energies. It is thus easy to see that at no reasonable signal levels and rates, even with arrays with substantial gain, will the total rate due to cosmic-ray muons at great distances be large. Note that we ignored the complexities of long-range acoustic propagation in an ocean with a variable index of refraction. The conclusion of this paper is that the relative amount of acoustic noise in the ocean caused by cosmic-ray muons is negligible. (However, this does *not* say that special detectors could not observe large rates of acoustically detected muons.)

VI. ACOUSTIC RADIATION FROM CASCADES OF PARTICLES

Another important circumstance is the radiation of sound from energetic cascades of particles. The practical applications of this could be in the laboratory[19] or in the ocean.

Most cascades of elementary particles have similar characteristics. They grow rapidly in particle numbers and ionization, spreading out conically and then decay exponentially. Their cross-sectional distributions are characterized by a $1/\rho^2$ decrease of ionization per unit volume. No simple function has been derived relating these cascades to known input parameters (e.g., average transverse momentum, particle multiplicity, etc.). Most available results are for Monte Carlo studies which have been tested in various ways against experiment.[20] The following function approximates some of the behavior of hadronic cascades:

$$\frac{dE}{dV} = AEF_1(\rho)F_2(s)\ \mathrm{MeV/cm}^3 , \tag{56}$$

$A = 3.66\times 10^{-4} E^{0.375}$,

E = initial hadronic-particle energy (in GeV) > 100,

$$F_1(\rho) = \frac{\rho_0{}^2}{(\rho_0+\rho)^2} \exp - \frac{(\rho+\rho_0)^2}{2\rho_m{}^2} ,$$

$F_2(s) = s^{\alpha} e^{-s}$,

$\rho_0 = r_0 s$,

$\rho_m = r_m s$,

$s = z/\lambda$,

$\alpha = 2.993$,

z = axial distance from first interaction in cm,

$\lambda = 14.2 \ln E$,

$$r_0 = \begin{cases} 0.045(18.4 - \ln E)\ \mathrm{cm} , \\ 0.1\ \mathrm{cm\ if}\ E > 9.8\times 10^{16}\ \mathrm{eV} , \end{cases}$$

$r_m = 160$ cm.

This function approximates the correct behavior in water, as well as other materials, roughly, by scaling the attenuation length λ by the ratio of absorption lengths in the materials and the radial factors r_0 and r_m by the Moliere lengths. The energy dependence is approximate, as is the normalization constant (A). No guarantees are made about the accuracy of this function particularly when extrapolated to high energies. It would be useful to have such a function carefully fit to cascade Monte Carlo results, particularly with respect to the sensitivity to various models used to extrapolate hadronic interaction characteristics to ultrahigh energies. However, the author believes that the function will be adequate for a first attempt at calculating the acoustic radiation at substantial distances from such cascades. For the very near field there will be sensitivity to details, plus at energies below roughly 10-TeV fluctuations (substantial) from shower to shower should really be taken into account. At higher energies the statistics will be good but the dominant uncertainty will be the length of the cascade.

We can identify four zones in the radiation pattern as a function of distance from the cascade axis:

(1) Very near field. Within a few cascade attenuation lengths (λ) of the cascade the behavior will be difficult to calculate.

(2) Near field. The pressure wave falls off as $1/\sqrt{r}$, as from a line of radiation. The radiation is contained in a cylinder of height $n\lambda$, where $n \sim 5$.

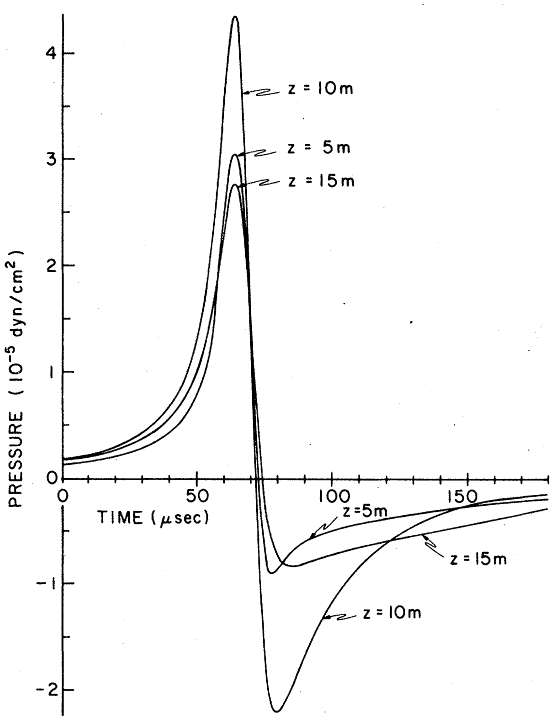

FIG. 4. Acoustic radiation from a 10^{16}-eV cascade in sea water with model described in text. Pressure pulses are shown at three locations 400 M distant from the cascade axis. At distances of several kilometers the pulses (within the beam width) will approach a common shape.

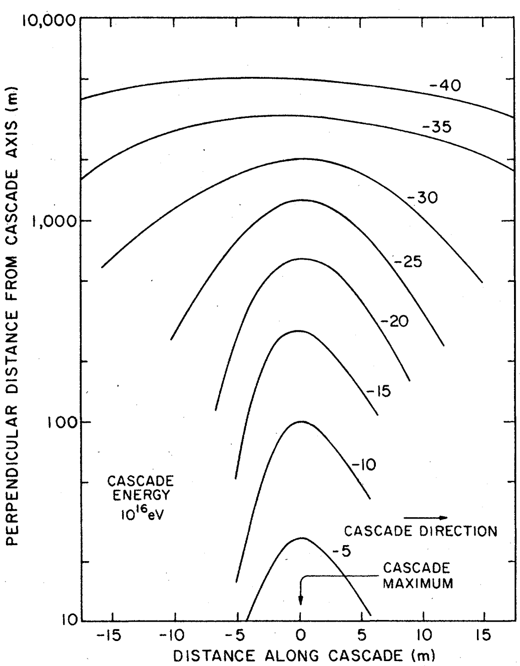

FIG. 5. Contours of constant inherent maximum signal-to-noise ratio for a 10^{16}-eV cascade in fresh water at 11°C.

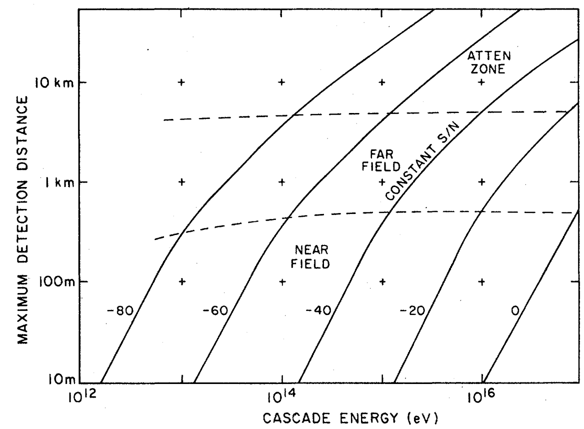

FIG. 6. Maximum detection distance versus energy for various signal-to-noise ratios.

(3) Far field. The fall of pressure with distance is now as $1/r$ and contained in a zone of angular width ρ_0/λ.

(4) Attenuation zone. Attenuation now takes effect and speeds the fall of pressure with distance to $1/r^2$. Note that the angular width now must increase in compensation because the apparent source size is dominated by the medium. The angular zone is roughly

$$(rc/\omega_0)^{1/2}/\lambda .$$

Notice also that the signal-to-noise ratio falls off only an extra $\frac{1}{2}$ power in r in this region [see Eq. (27)].

The same computer program as that described in

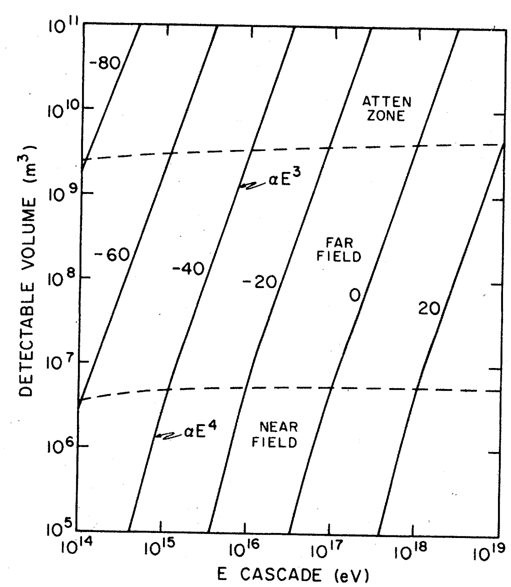

FIG. 7. Volume contained inside a given signal-to-noise ratio limit versus energy.

Sec. IV has been used to calculate pulses from cascades and to generate contour plots of pressure and signal-to-noise ratio. Figure 4(a) shows pressure pulses from a 10^{16}-eV cascade at 400 m along the perpendicular to the peak on the cascade axis. Figures 4(b) and 4(c) show the pulse as received ± 10 m from this point, parallel to the cascade axis. One sees a sensitivity to position, which may be used to unambiguously determine the cascade sense of motion. Figure 5 presents a plot of contours of constant (inherent maximum) signal-to-noise ratio for a 10^{16}-eV cascade. Figure 6 contains a plot of contours of constant signal-to-noise ratio on an energy versus maximum detection distance plot. Notice that the breaks into far and attenuation regions are gentle and only slowly varying with energy, occurring at about 400 m and 4 Km, respectively. Finally, most relevant for the DUMAND project, Fig. 7 gives the effective volume versus cascade energy for various signal-to-noise ratio limits. This is the volume within which such a cascade may be heard with signal-to-noise ratio greater than the stated value. There are many uncertainties in these calculations, but the behavior with energy is inescapable. The volume increases nearly linearly with the cube of the energy out to spectacular values of "insonification" volume. One must be careful because of the assumption of thermal noise and an infinite homogeneous ocean. Moreover, at great distances the attenuation is substantially greater than that predicted by an extrapolation of simple frequency-squared dependence from high frequencies downwards. These calculations represent upper limits for signal-to-noise ratios at kilometer distances in the ocean. (The temperature of 11℃ in fresh water corresponds to about 4℃ in salt water in the deep ocean in terms of the coefficient of bulk thermal expansion.)

SUMMARY

We have shown that acoustic radiation from atomic particles traversing liquid media can be usefully treated as the time-domain addition of the microscopic pulses from the ionization region. One need not know the details of the radiation on the particle scale so long as it approximates that due to point heating of the medium (i.e., no microbubbles). At most conceivable observation distances the temporal structure of the pressure pulse will be controlled by the characteristics of sound propagation in the medium.

Using the techniques developed herein, applications have been made to various distributions including the two situations of greatest current interest, the line radiation from heavy ions and the more complex radiation from a nuclear cascade. Perhaps the most striking result is the lack of a sharp cutoff of attenuation with this kind of radiation which leads to a power-law decrease (rather than an exponential decrease) with distance. This suggests that detection of particles at distances far into the attenuation region may be possible.

Further work is required (and is in progress) to account for variations of the attenuation coefficient from exact proportionality to the square of the frequency as well as better approximations to the ionization distributions of both cascades of particles and around individual particle trajectories. As yet, there is no experimental evidence in the U. S. for any mechanism other than thermoacoustic as used herein. Observation of microbubble production or other phenomena would be exciting and require a new analysis. (It should be added that we do have one piece of evidence not consistent with the simple thermoacoustic picture.[21])

ACKNOWLEDGMENTS

While the approach of this paper is largely my own, I owe thanks to Ted Bowen, Hugh Bradner, and Antares Parvulescu for many discussions and ideas. Without the pioneering thought of G. Askarjan, T. Bowen, and B. Dolgoshein and the enthusiasm of the DUMAND organization, this work would not have taken place. I also want to thank Fred Reines for his substantial help and for obtaining a grant from the office of the President of the University of California, David Saxon, which supported my research during the period that this work was largely completed. Some of the early computer calculations were aided by H. Bradner's NSF Contract No. EAR 76-84324 at University of California, San Diego. Jonas Schultz has also aided substantively, as have other colleagues at University of California, Irvine. The bulk of the computer calculations were supported by the U. S. Energy Research and Development Administration, Contract No. EY 76-S-03-0034-PA149. I want to acknowledge the help of Robin Snider and Craig Wuest in the later stages of the computer calculations and of Shirley Eisley in preparing the manuscript.

*On leave from the University of Wisconsin, Madison, Wisconsin.

[1]The most recent experimental activity in the United States is documented in the following papers: (a) T. Bowen *et al.*, in *Proceedings of the 1976 DUMAND Summer Workshop, Honolulu*, edited by A. Roberts (Fermilab, Batavia, Illinois, 1977), p. 547: (b) T. Bowen *et al.*, *ibid.*, p. 559; (c) L. R. Sulak *et al.*, in *Leptons and Multileptons*, proceedings of the XII Rencontre de Moriond, Flaine, 1977, edited by J. Trân Thanh Vân (Editions Frontières, Paris, 1977); (d) J. G. Blackinton *et al.*, J. Acoust. Soc. Am. 61, [illegible] (1977); (e) L. R. Sulak *et al.*, in *Neutrino* '77, proceedings of the International Conference on Neutrino Physics and Neutrino Astrophysics, Baksan Valley, U.S.S.R., edited by M. A. Markov *et al.* (Nauka, Moscow, 1978), Vol. 2, p. 350; (f) T. Bowen *et al.*, in *Proceedings of the XV International Conference on Cosmic Rays, Plovdiv, Bulgaria, 1977* (Bulgarian Acad. of Sciences, Plovdiv, 1977), Paper MN-71; (g) T. Bowen, B. Pifer, P. Polakos, H. Bradner, T. Armstrong, H. Baranger, M. Bregman, M. Levi, D. Mael, J. Strait, L. Sulak, A. Parvulescu, W. V. Jones, and J. Learned [Nucl. Instrum. Methods (to be published)].

[2]Recent work in the U.S.S.R. is reported in the following and references: (a) V. D. Volovik *et al.*, in Proceedings of the IX USSR Acoustics Conference, Moscow, 1977 (unpublished); (b)V. P. Volovik, V. I. Kobizskos, and G. F. Popov, Izv. Akad. Nauk SSSR, Ser. Fiz. 40, 1065 (1976) [Bull. Acad. Sci. USSR, Phys. Ser. 40, 164 (1976)]. It should be noted that there appear to be serious contradictions between the work of Ref. 1 and the work referred to above. In particular, the Soviet investigators find pulse amplitudes larger than the U. S. workers and they find evidence for microbubble production and other mechanisms while the U. S. workers, as yet, find only the thermoacoustic mechanism assumed in this article.

[3]Early experimental work in the U. S., apparently motivated by a study of sources of impulsive noise in gravitational radiation detectors, is reported in B. L. Beron *et al.*, IEEE Trans. Nucl. Sci. 17, 65 (1970); B. L. Beron and R. Hofstadter, Phys. Rev. Lett. 23, 184 (1969); R. M. White, J. Appl. Phys. 34, 3559 (1963).

[4]The first published suggestion of the use of charged elementary particles to produce sound is believed by this author to be by G. A. Askarjan, At. Energ. 3, 152 (1957) [Sov. J. At. Energy 3, 921 (1957)]. The first example of which this author is aware of an attempt to hear a charged-particle interaction was by L. Alvarez putting a small slug of uranium to his ear when close to a nuclear reactor during the early 1940's. He reported no signal (personal communication). Finally, the author believes that the first suggestion of the utility of acoustic radiation for detection of extremely high-energy interactions was by T. Bowen at a DUMAND meeting during the Fourteenth International Conference on Cosmic Rays, Munich, 1975. This suggestion was separately followed up by Bowen and Dolgoshein, who made independent proposals at the 1976 DUMAND summer study: (a) T. Bowen, in *Proceedings of the 1976 Dumand Summer Workshop, Honolulu* [Ref. 1(a)], p. 523. A corrected version of this work appears in *Proceedings of the XV International Conference on Cosmic Rays, Plovdiv, Bulgaria, 1977* [Ref. 1 (f)], Paper MN-73; (b) B. A. Dolgoshein, in *Proceedings of the 1976 Dumand Summer Workshop Honolulu* [Ref. 1 (a)], p. 553; (c) G. A. Askerjan and B. A. Dolgoshein, Lebedev Physical Institute of the U. S. S. R. Academy of Sciences, Moscow, 1976, Report No. 160 (unpublished).

[5]S. Hanish, Acoustics Div., U. S. Naval Research Laboratory, report (unpublished).

[6]Related theoretical work has had to do with the absorption of energy from lasers. A summary of some of this work will be found in H. Bradner's summary (in *Proceedings of the 1976 DUMAND Summer Workshop, Honolulu* [Ref. 1 (a)], p. 517) and references therein. Of greatest relevance are the papers of P. Westervelt and R. Larsen, J. Acoust. Soc. Am. 54, 121 (1973) and C.-L. Hu, *ibid.* 46, 728 (1969). The net observed pulse being proportional to the time derivative of the received density of pulses from heating centers can be deduced from the Westervelt and Larsen paper where $\cos\theta = 0$.

[7]The notation and presentation of J. Markham, R. Beyer, and B. Lindsay, Rev. Mod. Phys. 23, 353 (1951), is used throughout Sec. II.

[8]F. V. Hunt, in *American Institute of Physics Handbook*, Third edition, edited by Dwight E. Gray *et al.* (McGraw-Hill, New York, 1972), Chap. 3, p. 37 *et seq.*

[9]P. Morse and K. Ingard, *Theoretical Acoustics* (McGraw-Hill, New York, 1968).

[10]P. Morse and K. Ingard, *Theoretical Acoustics* (McGraw-Hill, New York, 1968), pp. 323 and 324.

[11]W. Davenport and W. Root, *Random Signals and Noise* (McGraw-Hill, New York, 1958), Chap. 11.

[12]R. H. Mellen, J. Acoust. Soc. Am. 24, 478 (1952); D. E. Ezrow, *ibid.* 34, 550 (1962); F. V. Hunt, Ref. 8, Chap. 3, pp. 65–68.

[13]In order to "prewhiten" the thermal noise we integrate in the time domain which is equivalent to multiplication by ω^{-1} in the frequency domain. More about this can be found in Bowen's report in the *Proceedings of the La Jolla Workshop on the Acoustic Detection of Neutrinos* La Jolla, California, edited by H. Bradner (unpublished).

[14]Ray Hagstrom of LBL, personal communication, thesis (unpublished). Also see P. B. Price, E. K. Shirk, W. Z. Osborne, and L. S. Pinksky, in *Proceedings of the Fourteenth International Conference on Cosmic Rays, Munich, 1975,* edited by Klaus Pinkau (Max-Planck-Institut, München, 1975), Vol. 12, p. 4033. For a discussion of dE/dx see L. C. Yuan and C. S. Wu, *Methods of Experimental Physics* (Academic, New York, 1961), part A, Sec. 1.1.

[15]*American Institute of Physics Handbook* (Ref. 8), p. 2-121.

[16]A. G. Wright, J. Phys. A: Math. Nucl. Gen. 7, 2085 (1974).

[17]A. Chudakov, *et al.*, in *Proceedings of the 1976 DUMAND Summer Workshop, Honolulu* [Ref. 1 (a)], p. 318.

[18]M. Thompson, R. Thornley, M. Whalley, and A. Wolfendale, in *Proceedings of the XV International Conference on Cosmic Rays Plovdiv. Bulgaria, 1977* [Ref. 1 (f)], Vol. 6, p. 21 (Paper MN-7). A general introduction can be found in A. W. Wolfendale, *Cosmic Rays at Ground Level* (The Institute of Physics, London, 1973).

[19]A. Roberts *et al.*, Proposal for Experiment E-528 at Fermilab, 1977 (unpublished).

[20]See cascade profiles in W. V. Jones, See Rev. 1 (a), p. 591, and G. Askarjan, B. Dolgoshein, Lebedev Report No. N160 (unpublished).

[21]As discussed in Ref. 1(g), the pressure amplitude does not go to zero in fresh water at 4° C (β crosses zero at this temperature), but nearer 5.9 ± 0.2°C. Impurities and microbubble radiation should lower rather than raise this value. P. Westervelt of Brown University has suggested (personal communication) that this is due to the rapidity of energy deposition not coupling to all energy states of the medium.

[22]*International Critical Tables* edited by E. W. Washburn (McGraw-Hill, New York, 1929). See particularly Vol. V, pp. 79–117 and Vol. VI, pp. 461–468.

[23]*Handbook of Tables for Applied Engineering Science* edited by R. E. Bolz and G. L. Tuve (CRC Press, Cleveland, Ohio, 1976).